Citation: Molecular Therapy—Nucleic Acids (2013) 2, e107; doi:10.1038/mtna.2013.37

www.nature.com/mtna

Dimeric DNA Aptamer Complexes for High-capacity–targeted Drug Delivery Using pH-sensitive Covalent Linkages

Olcay Boyacioglu[1], Christopher H Stuart[1,2], George Kulik[1] and William H Gmeiner[1,2]

Treatment with doxorubicin (Dox) results in serious systemic toxicities that limit effectiveness for cancer treatment and cause long-term health issues for cancer patients. We identified a new DNA aptamer to prostate-specific membrane antigen (PSMA) using fixed sequences to promote Dox binding and developed dimeric aptamer complexes (DACs) for specific delivery of Dox to PSMA$^+$ cancer cells. DACs are stable under physiological conditions and are internalized specifically into PSMA$^+$ C4-2 cells with minimal uptake into PSMA-null PC3 cells. Cellular internalization of DAC was demonstrated by confocal microscopy and flow cytometry. Covalent modification of DAC with Dox (DAC-D) resulted in a complex with stoichiometry ~4:1. Dox was covalently bound in DAC-D using a reversible linker that promotes covalent attachment of Dox to genomic DNA following cell internalization. Dox was released from the DAC-D under physiological conditions with a half-life of 8 hours, sufficient for *in vivo* targeting. DAC-D was used to selectively deliver Dox to C4-2 cells with endosomal release and nuclear localization of Dox. DAC-D was selectively cytotoxic to C4-2 cells with similar cytotoxicity as the molar equivalent of free-Dox. In contrast, DAC-D displayed minimal cytotoxicity to PC3 cells, demonstrating the complex displays a high degree of selectivity for PSMA$^+$ cells. DAC-D displays specificity and stability features that may be useful for improved delivery of Dox selectively to malignant tissue *in vivo*.

Molecular Therapy—Nucleic Acids (2013) **2**, e107; doi:10.1038/mtna.2013.37; published online 16 July 2013
Subject Category: Aptamers, ribozymes and DNAzymes

Introduction

Cell-specific delivery of cytotoxic drugs *via* passive[1] and active targeting[2] is an important objective in order to improve cancer chemotherapy.[3] Successful targeting requires the targeting vehicle to have appropriate dimensions for tumor localization *via* the enhanced permeability and retention effect[4] and to bind with high affinity to an antigen that is specifically expressed by targeted cells. Successful drug delivery *via* a targeted approach must meet additional requirements regarding the stability of the drug complex–drug must be retained in the complex during targeting which may take several hours, but released from the complex after binding to the targeted cell. Drug delivery should also be efficient, releasing multiple drugs for each successfully targeted complex. There is a strong need for new targeted drug delivery approaches that display stability with high payload delivery.

Prostate-specific membrane antigen (PSMA) is of interest for selective delivery of therapeutics for cancer treatment as a consequence of its elevated expression on the apical plasma membrane[5] of prostate cancer (PCa) cells and in endothelial cells of vasculature from diverse malignancies. PSMA is an exopeptidase[6] with folate hydrolase and NAALADase (N-acetylated α-linked acidic dipeptidase) activities. PSMA also associates with the anaphase-promoting complex and its expression may promote aneuploidy.[7] PSMA is expressed by prostate epithelial cells,[8] however, elevated PSMA expression occurs in advanced PCa, including bone metastases[9] and PSMA expression levels are an independent predictor of PCa recurrence.[10] PSMA is also expressed in vasculature[11] from many different cancers including a high percentage of bladder,[12] gastric, and colorectal,[13] as well as hepatocellular, renal, breast, and ovarian cancer.[6] PSMA is expressed as a dimer,[14] and dimerized ligands targeting the PSMA dimer display improved activity relative to monovalent ligands.[15]

The restricted expression of PSMA has resulted in numerous attempts to both image and treat cancer with PSMA-targeted diagnostic and therapeutic modalities. Three classes of molecules have been most frequently employed in these targeted applications: monoclonal antibodies such as J591, RNA aptamers such as A10-3, and small molecule inhibitors of PSMA enzymatic activity. Radiolabeled conjugates of J591 are being investigated for treatment of advanced PCa[16] and have been utilized for cancer imaging. PSMA inhibitors have been used to deliver theranostic nanoparticles to cancer cells.[17] The A10-3 RNA aptamer to PSMA has been used to deliver diverse therapeutic modalities selectively to cancer cells including cisplatin,[18,19] functionalized nanoparticles,[20] a micelle-encapsulated PI3K inhibitor,[21] as well as toxins[22], and small interfering RNA.[23,24] Aptamer targeting of PSMA may be particularly beneficial for delivery of anticancer drugs that have serious systemic toxicities, such as doxorubicin (Dox). Dox is among the most widely used chemotherapy drugs, however, treatment results in a serious, occasionally lethal cardiotoxicity that may manifest years after treatment, necessitating the development of selective delivery approaches.

[1]Department of Cancer Biology and Program in Molecular Medicine, Wake Forest School of Medicine, Winston-Salem, North Carolina, USA; [2]Program in Molecular Medicine and Translational Science, Wake Forest School of Medicine, Winston-Salem, North Carolina, USA. Correspondence: William H Gmeiner, Department of Cancer Biology, Wake Forest School of Medicine, Winston-Salem, North Carolina 27157, USA. E-mail: bgmeiner@wakehealth.edu
Keywords: aptamer; chemotherapy; prostate cancer; prostate-specific membrane antigen
Received 4 April 2013; accepted 30 May 2013; advance online publication 16 July 2013. doi:10.1038/mtna.2013.37

The current approaches to Dox delivery using RNA aptamers have several limitations that may be overcome to improve treatment outcomes. Current RNA aptamers are costly to produce, require modified nucleotides for nuclease stability and Dox is generally noncovalently associated with the aptamer. Noncovalent complexes of Dox with duplex DNA have limited stability with half-lives of only a few minutes (or less) and it is unlikely that noncovalent complexes of Dox with aptamers would be sufficiently stable for optimal *in vivo* activity. Here, we report a new strategy for improved targeted delivery of Dox to PSMA$^+$ cancer cells using a novel dimeric DNA aptamer complex bound to Dox through a pH-sensitive linker. PSMA is expressed on the plasma membrane as a dimer, and dimerized ligands targeting PSMA display improved activity relative to monovalent ligands.[15] We formed a dimeric aptamer complex (DAC) to take advantage of the dimeric nature of PSMA. As our goal was to efficiently deliver multiple Dox per DAC, we included 5′-dCpG, the preferred binding site for Dox, interspersed in the primers used for PCR amplification during SELEX to permit Dox-binding motifs to be retained in the final DNA aptamer sequence (**Figure 1**). We employed a novel strategy in which the priming sequences were imperfectly matched to fixed sequences within the template, permitting aptamer length to vary during the selection process. We identified a 48 nucleotide DNA aptamer (SZTI01, **Supplementary Figure S1**) using an affinity matrix consisting of the extracellular domain of human PSMA.

Results

Thermal stability of DACs

A key design feature for our strategy to deliver Dox to PCa cells was the formation of a duplex DNA "bridge" linking the two DNA aptamers in the DAC (**Figure 1**). The bridging DNA duplex is designed to be sufficiently thermally stable such that the DAC remains intact under physiological conditions for times sufficient for aptamers to localize specifically to targets *in vivo*, and includes a preferred site for Dox binding (CpG). The fixed sequences used during the aptamer selection process also included preferred sites for Dox binding that are included in the final DAC structure.

Thermal melting profiles were obtained for DACs with and without Dox modification to evaluate stability of these complexes and any effects Dox may have on thermal stability (**Figure 2**). The temperature-dependent ultraviolet (UV) melting profile for the dA_{16}:T_{16} DAC indicated some reduction in secondary structure at temperatures less than 30°C with initial dissociation of the dimeric complex at ~41 °C with a dissociation temperature of ~47 °C. While dissociation for this dimeric complex occurred above physiological temperature, increased stability would be preferred to promote long-term stability under physiological conditions. Further, the A-T duplex used to form this dimeric complex did not include a preferred Dox-binding sequence motif. We prepared an alternative DAC by appending GCCG and CGGC sequences to the 5′- and 3′-ends of the A_{16}:T_{16} DNA duplex-forming sequences (**Figure 1**). The resulting DAC displayed a dissociation temperature of ~58 °C, thus displaying stability suitable for further development. Covalent modification of DAC with Dox (DAC-D) further enhanced complex stability, and the DAC-D complex displayed minimal change in absorbance for temperatures lower than the melting temperature consistent with Dox stabilizing DAC structure (**Figure 2a**).

The secondary structure and thermal stability of DAC were further investigated using circular dichroism spectroscopy (**Supplementary Figure S2**). The DAC complexes displayed circular dichroism spectra typical of B-form DNA with a maximum at 283 nm and a minimum at 248 nm consistent with the tail-forming sequences forming the target structures. Covalent modification with Dox in the DAC-D complex has no discernible effect on overall secondary structure for the complex although a slight sharpening in the peaks was noted. The DAC-D complex displayed less sensitivity to increased temperature relative to DAC and DAC + Dox indicating covalent modification with Dox stabilizes the overall complex.

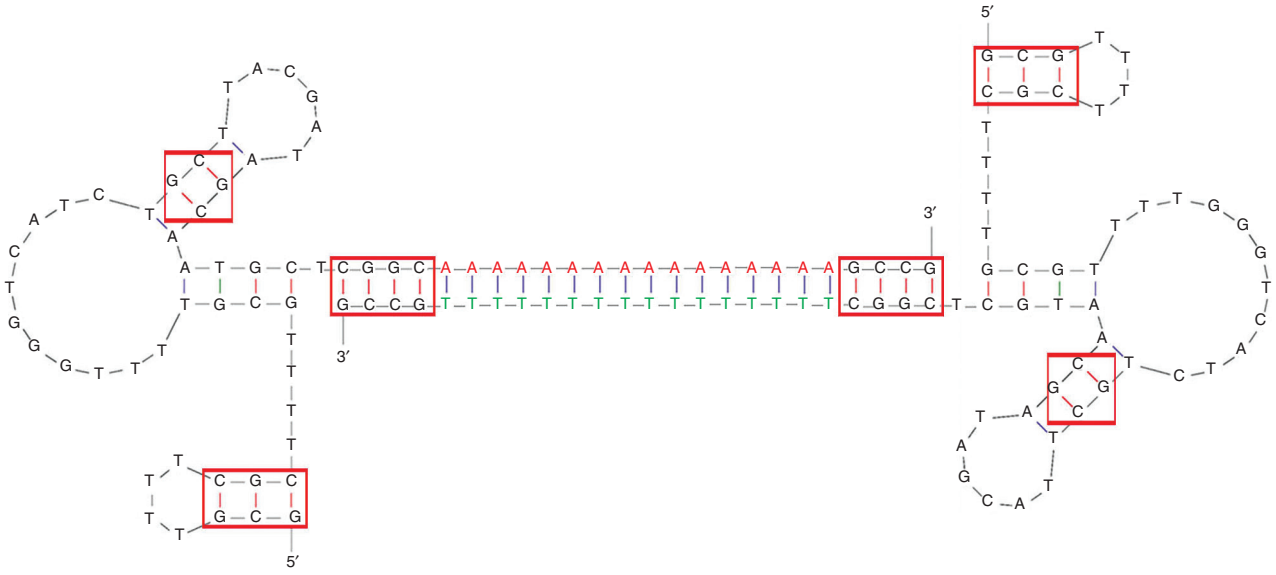

Figure 1 Secondary structure of the dimeric aptamer complex containing CpG sequences appended to the ends of the dA_{16} (red bases) or T_{16} (green bases). Red boxes indicate potential doxorubicin-binding sites.

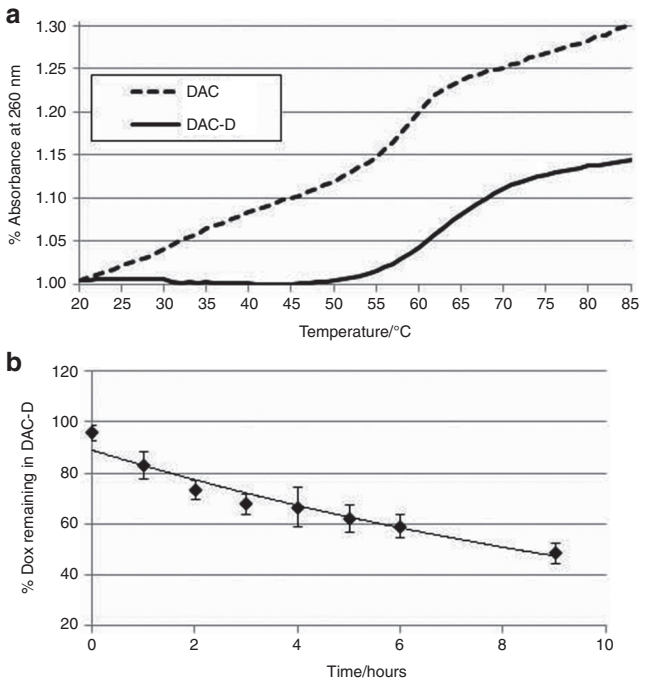

Figure 2 Physical characterization of DAC and DAC-D. (**a**) The T_m of DAC and DAC-D was determined by measuring the ultraviolet absorbance at 260 nm and by heating the samples at 0.7 °C/minute. (**b**) Dox fluorescence was measured by exciting the sample with a 532 nm laser and reading the emission at 580 nm. The calculated half-life of transfer from DAC-D was found to be 8.27 hours. Error bars represent mean ± SD. DAC, dimeric aptamer complex; DAC-D, dimeric aptamer complex with doxorubicin.

Formation and dissociation of covalent Dox conjugates

The duplex DNA-binding motif stabilizing the DAC has the potential for binding two equivalents of Dox per complex. In addition, the DNA aptamers comprising the complex contained other CpG sites for potential Dox binding (**Figure 1**). We formed a covalent complex between the DAC and Dox (DAC-D) by mixing the dimeric complex with a fourfold excess of Dox in the presence of formaldehyde. We formed covalent linkages at 4:1 stoichiometry (**Supplementary Figure S3**; **Supplementary Table S1**) and evaluated Dox transfer from the resulting covalent complex (DAC-D) in which Dox fluorescence is effectively quenched to an excess of a 25mer DNA hairpin in which Dox fluorescence is less effectively quenched. These studies revealed the half-life for Dox covalently bound in DAC-D *via* formaldehyde was >8 hours (**Figure 2b**), while the dissociation of the noncovalent complex was too rapid to measure using this assay, but is fully dissociated in ≤5 minutes. These studies indicated that covalent attachment of Dox results in formation of a complex with increased retention of Dox that is well suited for drug delivery applications *in vivo*.

PSMA-specific uptake of dimeric complexes

The selective delivery of Dox to PSMA$^+$ cells requires binding and ideally internalization of the complex. To evaluate to what extent the DAC was specific for binding and internalization into PSMA$^+$ cells, we compared internalization of the complex in PSMA$^+$ C4-2 cells and PSMA-null PC3 cells using confocal microscopy and flow cytometry. The component of the dimeric complex containing dA_{16} single-stranded (ssDNA) was labeled with Quasar 570, while the component with T_{16} ssDNA was labeled with Quasar 670 permitting simultaneous detection and visualization of each aptamer component. Confocal microscopy revealed minimal uptake of either fluorescently labeled aptamer into PC3 cells, however, strong signal was observed for each fluorescent aptamer signal in PSMA$^+$ C4-2 cells (**Figure 3**). Further, fluorescence emitted from each of the two aptamers was completely colocalized consistent with uptake and retention of the DAC in dimeric form. Fluorescence emitted from the aptamer complexes appeared punctate, with nuclear exclusion, consistent with endosomal localization of the DAC which was confirmed by colocalization with the endosomal marker fluorescein isothiocyanate–dextran (**Figure 4**). Flow cytometry also confirmed specificity of DAC for PSMA$^+$ C4-2 cells (**Supplementary Figure S4**). Preincubation of C4-2 cells with J591 PSMA-specific monoclonal antibody attenuated DAC uptake consistent with PSMA-specific internalization (**Figure 5a**).

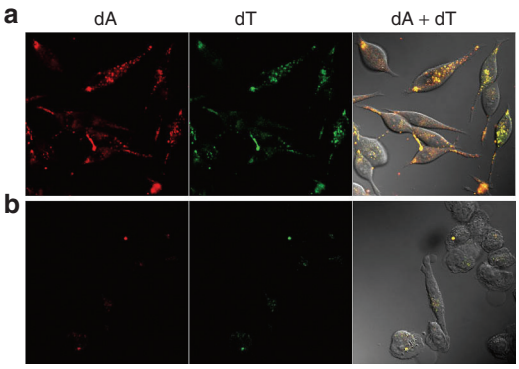

Figure 3 Cells were incubated with 1 µm of dimeric aptamer complex (DAC) for 2 hours before being fixed and imaged. Confocal microscopy shows DAC binds to and is internalized by (**a**) the prostate-specific membrane antigen (PSMA)$^+$ cell line C4-2, but not by (**b**) the PSMA-null cell line PC3. Colocalization studies (dT_{16} Quasar 570/green, dA_{16} Quasar 670/red) confirm DAC internalization as a dimer in C4-2 cells.

PSMA-specific delivery of Dox

The serious toxicities associated with Dox treatment indicate that premature release of Dox from targeting vehicles is likely to be therapeutically detrimental. In this regard, noncovalent complexes of Dox with DNA have demonstrated improved toxicity profiles relative to free-Dox,[25] however covalent linkage of Dox with a targeted DNA vehicle should markedly enhance efficacy and reduce systemic toxicities by limiting Dox dissociation while in circulation. We devised a strategy to covalently attach Dox to the DAC using formaldehyde, a strategy previously shown to promote covalent complex formation of Dox with genomic DNA.[26] The specific delivery of Dox to PSMA$^+$ cells using DAC-D was evaluated using confocal microscopy (**Figure 5b**). While noncomplexed Dox readily accumulated in the nuclei of both PC3 and C4-2 cells, Dox delivered using DAC-D internalized nearly exclusively into C4-2 cells with minimal accumulation in PC3 cells. Dox fluorescence was exclusively nuclear, while the aptamer

fluorescent signal from DAC-D displayed nuclear exclusion consistent with Dox becoming dissociated from the DAC-D following cellular internalization. These results are consistent with Dox becoming dissociated in the acidic environment of the endosome following cell uptake of DAC-D followed by nuclear localization of Dox. The results demonstrate PSMA-specific uptake of the DAC-D complex with nuclear delivery of Dox.

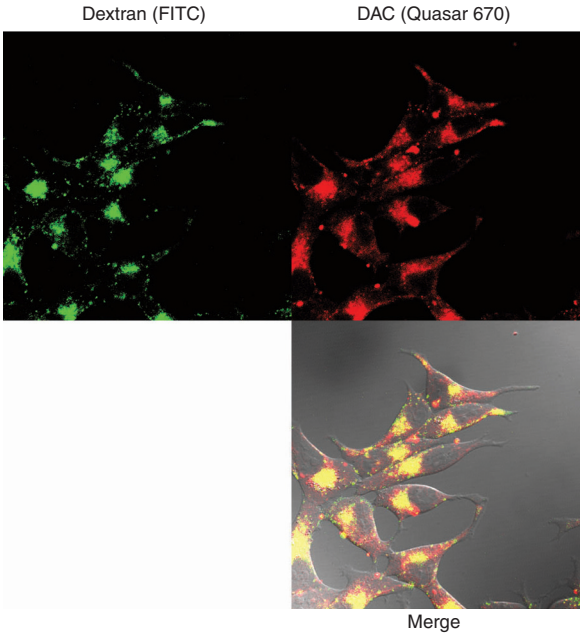

Figure 4 Cells were incubated with 1 mg/ml FITC–dextran (70 kDa) and 1 µmol/l DAC for 2 hours before fixation and imaging. Colocalization of FITC–dextran (70 kDa; green) with DAC (red) in C4-2 cells confirms the DAC enters the cell through endosomes. DAC, dimeric aptamer complex; FITC, fluorescein isothiocyanate.

PSMA-dependent selective cytotoxicity

Paramount to targeted drug delivery is selective cytotoxicity towards targeted cells with minimal damage to nontargeted cells. The specificity of DAC-D for PSMA$^+$ cells was evaluated using cell viability assays in PC3 and C4-2 cells. The results are shown in **Figure 6**. Free-Dox was highly cytotoxic to both PC3 and C4-2 cells consistent with the wide-spectrum activity previously reported (**Supplementary Figure S5**). In contrast, Dox delivery *via* DAC-D was highly cytotoxic towards C4-2 cells, but displayed greatly reduced cytotoxicity to PC3 cells. For example, at Dox concentrations that resulted in ~90% reduction in viability for free-Dox (2 µmol/l), the same amount of Dox delivered *via* DAC-D displayed greater than 80% potency towards targeted C4-2 cells and less than 50% of cytotoxic activity towards PC3 cells.

An especially challenging situation for targeted drug delivery occurs when targeted cells are in close proximity to nonmalignant cells as arises in metastases to vital organs. In this case, highly localized cytotoxicity is desirable. To simulate this challenging environment, we performed coculture of luciferase-transfected C4-2 cells (C4-2-luc) with PC3 cells and assessed the viability of each cell line in coculture independently (**Figure 6**). Preliminary studies demonstrated that C4-2-luc and C4-2 cells displayed no significant difference in viability in response to Dox or the DAC-D complex

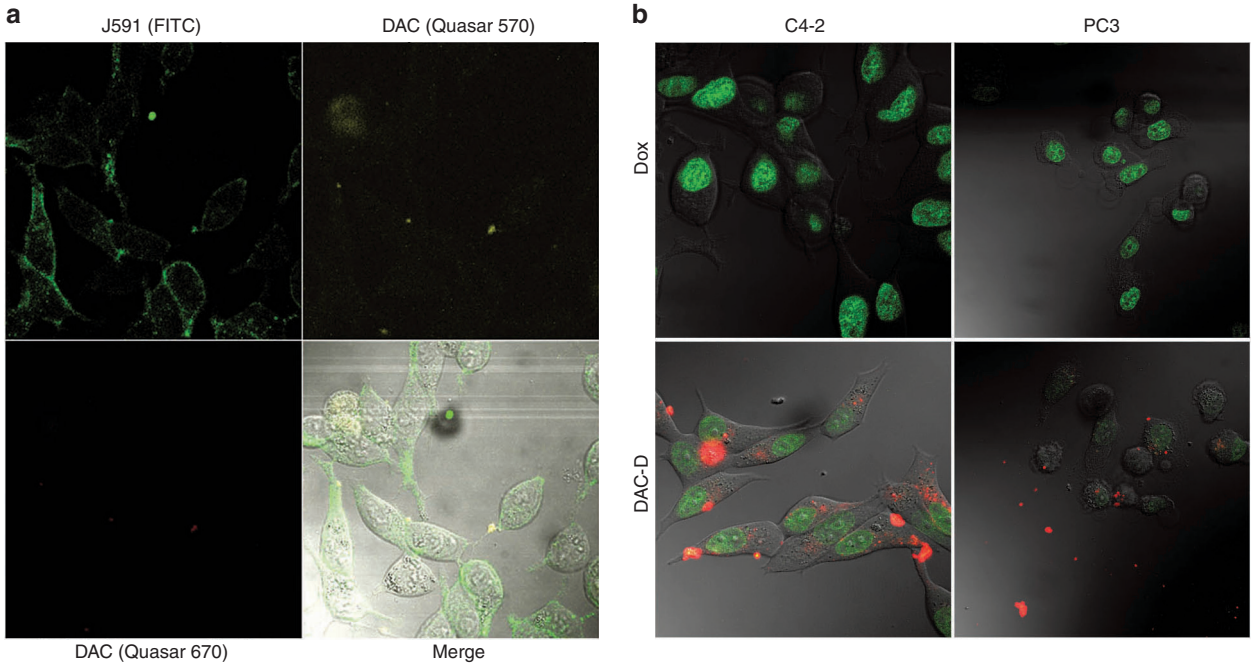

Figure 5 Specificity of DAC complexes for PSMA$^+$ cells. (**a**) C4-2 cells were incubated with the prostate-specific membrane antigen–specific antibody J591 for 30 minutes before washing and fixation using formaldehyde. Cells were then treated with DAC for 20 minutes and imaged using confocal microscopy. (**b**) Cells were incubated with either 1 µmol/l Dox, 1 µmol/l Dox premixed with 250 nmol/l DAC, or 250 nmol/l DAC-D (1 µmol/l Dox equivalent) for 2 hours before fixation and imaging. Dox shows nuclear localization in all cells. The use of DAC to deliver Dox results in reduced Dox delivery to PC3 cells. DAC, dimeric aptamer complex; DAC-D, dimeric aptamer complex with doxorubicin; Dox, doxorubicin; FITC, fluorescein isothiocyanate.

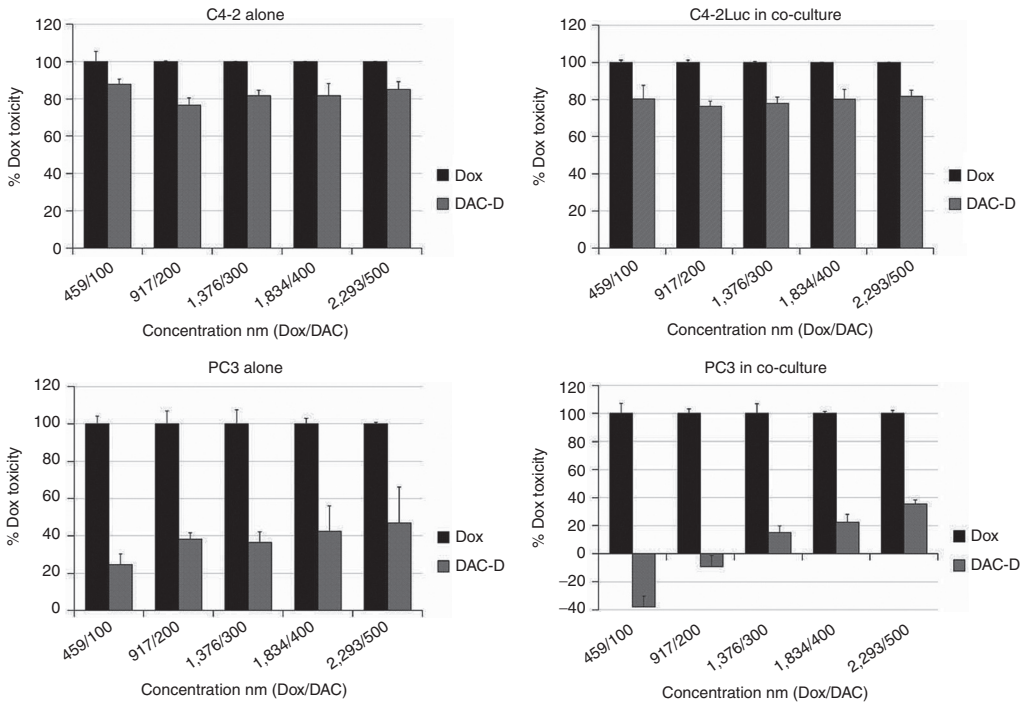

Figure 6 PC3 and C4-2 cells were incubated alone or in coculture and were treated with DAC-D, DAC + Dox, or free-Dox for 24 hours. Media was replaced and cells were allowed to grow for 48 hours before determining viability. Percentage of Dox retained was found by comparing the viability of DAC-D (or DAC + Dox) with Dox. There is no statistical difference between C4-2 cells alone versus C4-2 cells in coculture, however there is a significant reduction in cytotoxicity for PC3 cells in coculture versus PC3 cells alone ($P < 0.05$). Error bars represent mean ± SEM. DAC, dimeric aptamer complex; DAC-D, dimeric aptamer complex with doxorubicin; Dox, doxorubicin.

(**Supplementary Figure S5**). The response of C4-2-luc cells in coculture with PC3 cells was similar to C4-2 cells in monoculture with DAC-D retaining greater than 80% cytotoxicity in the mixed environment. In contrast, PC3 cells in coculture with C4-2-luc cells showed markedly decreased response to DAC-D relative to studies in monoculture ($P < 0.05$). The results are consistent with the DAC-D undergoing selective internalization into targeted PSMA$^+$ C4-2 cells, reducing the DAC-D available for nonspecific uptake into nontargeted PC3 cells.

Discussion

Aptamer-mediated delivery is a promising technology for improving the therapeutic index of cytotoxic drugs that cause serious systemic toxicities, such as Dox. We identified a new DNA aptamer to PSMA and developed a DAC to take advantage of PSMA being expressed as a dimer. Our objective was to use the DAC as a scaffold for high-capacity drug delivery. The process used for aptamer identification was designed to identify DNA sequences that included preferred Dox-binding sites (e.g., 5′-CpG). We also developed a process for covalent modification at the preferred binding sites with Dox resulting in a high-capacity (4:1) payload. The covalent linkage utilized is pH-sensitive releasing free-Dox in the acidic environment of endosomes following internalization into targeted cells. Released Dox migrates to the nucleus and binds genomic DNA interfering in replication and mitosis, while the DAC is retained in the cytosol. The resultant DAC-D complex is internalized selectively into PSMA$^+$ cells and is highly cytotoxic to these cells while displaying minimal effects to PSMA-null cells. Importantly, this high degree of selectivity is retained in the context of coculture experiments in which PSMA$^+$ cells retain full sensitivity to the targeted complex even while cocultured adjacent PSMA-null cells are not affected. It is anticipated that DAC-D complexes will be highly effective antitumor agents *in vivo* with minimal systemic toxicity.

DACs have potential advantages relative to monomeric aptamers for drug delivery applications in terms of target selection, target avidity, physical and chemical stability, higher payload capacity, improved pharmacokinetics, and utility if partly damaged–among other properties. The present studies utilized a DAC with both components targeting PSMA which is expressed as a dimer. The length of the 24 base pair DNA duplex connecting the component aptamers is approximately 70 Å which is similar to the dimensions of the PSMA dimer making it possible for the component aptamers to bind simultaneously, although optimization of DAC dimensions would be required to fully optimize simultaneous binding. The structure of the DAC utilized in the present studies was stable under physiologically relevant conditions and useful for high-capacity drug delivery with a 4:1 stoichiometry payload. In principle, additional Dox-binding sites can be included into the structure to further enhance drug delivery potential.

The chemical linkage used for covalent Dox attachment enables convenient synthesis with high yields and straightforward purification. While this approach is readily scaled for *in vivo* studies and eventual clinical applications, perhaps the most important advantage of using this chemistry for Dox delivery is that Dox is readily released from the DAC-D under moderately acidic conditions (pH <6) that occur in

endosomes following cellular internalization, or possibly in the tumor microenvironment. Dox released from endocytic DACs readily translocates to the nucleus and is capable of exerting cytotoxicity to a similar extent as free-Dox which acts *via* topoisomerase 2 poisoning. Formaldehyde released from the DAC-D upon acid-mediated dissociation has the potential to promote Dox binding to genomic DNA,[27,28] thus formaldehyde is not merely a passive chemical linkage, but may also potentiate genomic DNA binding of Dox released from the DAC-D delivery vehicle. This approach has advantages relative to strategies that use covalent linkers that lack this potential for enhancing genomic DNA binding by released Dox.

Aptamers may be prepared more cost effectively relative to monoclonal antibodies and are more amenable to chemical derivation for drug delivery applications. PSMA has emerged as a favored target for aptamer-mediated delivery of cytotoxic drugs and nanoparticles because of its elevated expression in advanced PCa and in the vasculature of diverse malignancies. The majority of studies described for PSMA targeting with aptamers have used variants of the A10 RNA aptamer.[22] While these studies have demonstrated target selectivity, there is a need for new aptamers that display improved targeting distinction and that retain the cytotoxic payload to a greater extent during delivery. We have identified a new DNA aptamer to PSMA, and developed a dimeric complex that displays a high degree of selectivity for $PSMA^+$ cells similar to the A10 RNA aptamer (**Supplementary Figure S6**).

Improved pharmacokinetic properties and reduced cardiotoxicity are important characteristics for Dox delivery that improves treatment outcomes for cancer patients. In this regard, the liposomal formulation, Doxil, has demonstrated decreased blood clearance and reduced cardiotoxicity relative to free drug. Doxil is not specifically targeted to malignant cells, and delivery that includes active targeting is expected to further increase treatment efficacy. The DAC-D described here has molecular weight (~45 kDa) suitable for prolonged retention in plasma as well as tumor localization *via* the enhanced permeability and retention and with specificity for malignant cells *via* PSMA targeting. Future studies will investigate the pharmacokinetic properties of DAC-D as well as systemic toxicities and efficacy towards *in vivo* models of cancer. Based on previous studies showing DNA delivery of Dox-reduced cardiotoxicity,[25] we expect DAC-D to have minimal cardiotoxicity. Ultimately, we expect DAC-D to prove useful for clinical management of cancer.

Materials and methods

DNA SELEX. Recombinant human PSMA extracellular domain (720 amino acids) was expressed from baculovirus (Kinakeet Biotechnology, Richmond, VA). The recombinant protein included a His-tag sequence that was used to form an affinity matrix using Talon beads which was then used in a DNA SELEX procedure to identify DNA aptamers to PSMA. DNA aptamers were selected from a library including a 47 nucleotide random sequence flanked by fixed sequences of 21 nucleotides each. The fixed sequences selected permit formation of short hairpins in the final aptamer that include stem regions with sequence elements favorable for Dox binding (underlined). The sequence for the random library was:

d<u>GCG</u>AAAA<u>CGC</u>AAAAGCGAAAA(N47)ACAGCAAT<u>CG</u>TAT<u>GC</u>TTAGCA

Initially, 8-µg ssDNA from the random library (307 pmol of DNA; 186 trillion sequences) was converted to double-stranded DNA (dsDNA) using a T7 fill-in reaction and amplified by PCR using primers that were imperfectly matched to the template.

5′ dGCGTTTTCGCTTTTGCGTTTT (forward)

5′ dAGCATTGCTATCGTAAGCAGA (reverse)

The 5′-primer was synthesized with a 5′-phosphate and the resulting dsDNA was converted to ssDNA using λ-exonuclease to selectively cleave the strand amplified with the phosphorylated primer. SELEX forward rounds were performed by adding 1 mg of PSMA bound to Dynabeads Talon (Invitrogen, Oslo, Norway) to 700 µl of binding buffer (100 mmol/l NaCl, 20 mmol/l Tris, 2 mmol/l $MgCl_2$, 5 mmol/l KCl, 1 mmol/l $CaCl_2$, 0.2% Tween-20, pH 8). The beads were removed using a Dynal magnet (Invitrogen) and were washed four times with binding buffer. At least 10 µg of ssDNA was annealed by heating to 95 °C followed by gentle cooling and was added to the PSMA matrix followed by vortexing and incubation for 1 hour at 37 °C with mild agitation. The supernatant was removed and 20 µl of 5 µmol/l 5′-phosphorylated primer was added to the beads and the mixture was heated to 95 °C for 5 minutes following which the beads were sequestered and the supernatant transferred to a clean microfuge tube and DNA converted to dsDNA using a primer extension reaction using T7 polymerase. DNA was collected by ethanol precipitation and then amplified by 10 cycles of PCR using a phosphorylated 3′-primer. The dsDNA was purified by gel electrophoresis followed by ethanol precipitation and then converted to ssDNA by treating 32–40 µg of dsDNA with λ-exonuclease for 30 minutes at 37 °C followed by ethanol precipitation. The resulting ssDNA was analyzed by gel electrophoresis and quantified by UV absorbance and used in a subsequent SELEX forward or counter round. Counter rounds differed from forward rounds by incubation with a magnetic bead matrix that did not contain PSMA and using the DNA that did not bind to the matrix for subsequent PCR amplification. A total of 10 forward and two counter rounds were performed. After the final SELEX round, ssDNA was converted to dsDNA using a T7 fill-in procedure and was cloned into a pGEM vector (Promega, Madison, WI) for sequencing. A single, 48 nucleotide sequence (SZTI01) was identified and used in subsequent studies.

$SZTI_{01}$: dGCGTTTTCGCTTTTGCGTTTTGGGTCATCTGC TTACGATAGCAATGCT

PSMA-specific aptamer synthesis. The DNA aptamer sequences were synthesized at either the University of Calgary (Calgary, Alberta, Canada) or IDT (Coralville, IA). Aptamers were reconstituted in sterile, nuclease-free H_2O at 100 µmol/l. DACs were prepared from aptamers that included either a dA_{16} or T_{16} single-stranded tail at the 3′-terminus (dA_{16}:T_{16} DAC) by mixing the two monomers at 1:1 ratio followed by heating to 95 °C and gentle cooling. The DAC used for these studies (unless otherwise indicated) included the sequences dCGGCA_{16}GCCG or dCGGCT_{16}GCCG. The secondary structure for the DAC calculated using m-fold is shown in **Figure 1**.

Synthesis of DAC-D complexes. The covalent complex of DAC-D was prepared by mixing 250 µl of a 50 µmol/l solution of the DAC with a Dox–formaldehyde solution prepared upon incubation of a 0.37% formaldehyde solution in Dulbecco's phosphate-buffered saline (PBS) without calcium or magnesium pH 7.4 with Dox. The reaction proceeded in a light-free manner at 4 °C for 48 hours. The solution was extracted once with 300 µl of phenol:chloroform followed by two additional extractions with 300 µl chloroform. The aqueous phase was then ethanol precipitated and the pellet rinsed 2× with 70% ethanol and once with absolute ethanol and dried under reduced pressure. The red pellet was resuspended in 100 µl dH_2O. Yields were typically >90% based on DNA recovery.

Determination of Dox:DNA ratios. DNA samples were prepared in dH_2O and absorbencies were measured from 200–800 nm using a Beckman Coulter DU-800 spectrophotometer (Beckman Coulter, Brea, CA). A standard curve of Dox was established between 1 and 10 µmol/l by using absorbencies at 494 nm at 85 °C. To assess the amount of Dox covalently bound to DNA, the samples were heated to 85 °C before measuring the absorbance at 494 and 260 nm. The 260 nm wavelength was used to determine the DNA content in the sample and to determine the Dox:DNA ratio.

Dox transfer from DAC-D. Samples of DAC-D or the noncovalent complex (DAC + D), or free-Dox 625 nmol/l were prepared in Dulbecco's PBS with or without a 100-fold (by weight) excess of a 25mer DNA and were incubated at 37 °C. Changes in fluorescence intensity were determined using a Typhoon-9210 variable mode imager with excitation set to 532 nm and the emission filter at 580 nm.

Temperature-dependent UV studies. Temperature-dependent UV absorption spectra were obtained using a Beckman Coulter DU-800 UV-Vis spectrophotometer. Samples of DAC, DAC-D, and DAC + D were prepared. The temperature was increased at a rate of 0.7 °C/minute over the range 20–85 °C and absorbance at 260 nm was measured for each sample (400 µl and 1 µmol/l) concentration.

Cell lines. The C4-2 cell line was a gift from Dr Elizabeth M Wilson (University of North Carolina, Chapel Hill, NC). C4-2-Luc cell line was generated by transfecting C4-2 cells with pTRE2hygro and firefly luciferase (PGL3). PC3 cells were purchased from cell and viral vector core laboratory at Wake Forest School of Medicine. All cells were maintained with RPMI 1640 (Gibco, Grand Island, NY) with 10% fetal bovine serum (Gemini Bio-Products, West Sacramento, CA). All cells were kept at 5% CO_2 at 37 °C.

Confocal microscopy. Cells were seeded at 20,000 cells/well in 8-well Lab-Tek II chambered #1.5 German Coverglass System (Thermo Fisher Scientific, Waltham, MA), and incubated at 37 °C under 5% CO_2 for 2 days. Cells were incubated with 1 µmol/l of DAC in which the dA_{16} aptamer was labeled with Quasar 570 at the 5′-terminus and the T_{16} aptamer was labeled with Quasar 670 dyes in RPMI medium with 10% fetal bovine serum for 2 hours at 37 °C. Cells were washed with fresh media and Dulbecco's PBS, followed by a 5 minutes fixation with 3.7% formaldehyde in Dulbecco's PBS. Cells were visualized using a Zeiss LSM510 confocal microscope (Carl Zeiss, Oberkochen, Germany). Cells were also incubated with 1 µmol/l of DAC-D (or the noncovalent DAC + D) for 2 hours. DACs were only labeled with Quasar 670 for these studies as the Quasar 570 emission would interfere with the Dox emission. Cells were washed, fixed, and imaged using identical procedures.

Flow cytometry. PC3 and C4-2 cells were incubated with 1 µmol/l of DAC for 2 hours at 37 °C. Dimers were fluorescently labeled with either Quasar 570 or 670 alone, or both. Cells were trypsinized and washed with PBS twice. Cells resuspended in PBS were analyzed to measure their intracellular fluorescence using the Accuri C6 flow cytometer (BD Biosciences, San Jose, CA).

Cytotoxicity measurements. PC3, C4-2, and C4-2-Luc cells were seeded at a density of 3,000 cells/well in 96-well plates and incubated at 37 °C under 5% CO_2. Next day, the cells were treated with Dox, DAC + Dox, or DAC-D for 24 hours. Next day the treatment was removed, cells were washed once with warm fresh media and incubated for another 48 hours in fresh media. Cell counts were measured indirectly by measuring the ATP amounts using CellTiter-Glo luminescent cell viability assay (Promega) according to the manufacturer's protocol. In coculture experiments, PC3 and C4-2-Luc cells were each seeded at a density of 1,500 cells/well in 96-well plates. Cocultured cells were treated with Dox, DAC + Dox, or DAC-D and cell viability was also measured using the CellTiter-Glo assay. Luciferase levels were measured for cocultures of PC3 and C4-2-Luc cells using a luciferase reporter assay system (Promega). PC3 and C4-2-Luc cells were seeded and treated as described above and the cells were lysed and luciferase activity was measured according to the manufacturer's protocol.

Supplementary material

Figure S1. The sequence of the SZTI01 aptamer.
Figure S2. Circular dichroism spectra were acquired at three temperatures (as indicated) at wavelengths 200–350 nm and a graph of the temperature-dependent reduction in ellipticity, which is less for DAC-D than DAC, is displayed.
Figure S3. A standard curve for Dox was established by measuring the absorbance of Dox at 494 nm at 85 °C.
Figure S4. Flow cytometry was performed by incubating cells with DAC for 2 hours before measuring the amount of fluorescence emitted by either Quasar 670 or Quasar 570 as a read-out for aptamer internalization.
Figure S5. Cells were treated with drugs for 24 hours.
Figure S6. Relative binding of the A10 RNA aptamer and SZTI01 to C4-2 cells is similar.
Table S1. Absorbance values for DAC-D complexes of different aptamer:Dox ratio.

Acknowledgments. Elizabeth M Wilson (University of North Carolina, Chapel Hill, NC) provided C4-2 cells. Stacy Trozzo and Patrick Guthrie helped with SELEX. Funding: DOD PCRP 093606 (W.H.G.) and National Institutes of Health-National Cancer Institute P30CA012197 (W.H.G.). The authors declared no conflict of interest.

1. Maeda, H (2012). Macromolecular therapeutics in cancer treatment: the EPR effect and beyond. *J Control Release* **164**: 138–144.
2. Byrne, JD, Betancourt, T and Brannon-Peppas, L (2008). Active targeting schemes for nanoparticle systems in cancer therapeutics. *Adv Drug Deliv Rev* **60**: 1615–1626.
3. Li, L, Sun, J, He, Z (2013). Deep penetration of nanoparticulate drug delivery systems into tumors: challenges and solutions. *Curr Med Chem* 2 May 2013 epub ahead of print <http://www.ncbi.nlm.nih.gov/pubmed/23651305>.
4. Erickson, HP (2009). Size and shape of protein molecules at the nanometer level determined by sedimentation, gel filtration, and electron microscopy. *Biol Proced Online* **11**: 32–51.
5. Christiansen, JJ, Rajasekaran, SA, Inge, L, Cheng, L, Anilkumar, G, Bander, NH *et al.* (2005). N-glycosylation and microtubule integrity are involved in apical targeting of prostate-specific membrane antigen: implications for immunotherapy. *Mol Cancer Ther* **4**: 704–714.
6. Denmeade, SR, Mhaka, AM, Rosen, DM, Brennen, WN, Dalrymple, S, Dach, I *et al.* (2012). Engineering a prostate-specific membrane antigen-activated tumor endothelial cell prodrug for cancer therapy. *Sci Transl Med* **4**: 140–186.
7. Rajasekaran, SA, Christiansen, JJ, Schmid, I, Oshima, E, Ryazantsev, S, Sakamoto, K *et al.* (2008). Prostate-specific membrane antigen associates with anaphase-promoting complex and induces chromosomal instability. *Mol Cancer Ther* **7**: 2142–2151.
8. Gong, MC, Chang, SS, Sadelain, M, Bander, NH and Heston, WD (1999). Prostate-specific membrane antigen (PSMA)-specific monoclonal antibodies in the treatment of prostate and other cancers. *Cancer Metastasis Rev* **18**: 483–490.
9. Mannweiler, S, Amersdorfer, P, Trajanoski, S, Terrett, JA, King, D and Mehes, G (2009). Heterogeneity of prostate-specific membrane antigen (PSMA) expression in prostate carcinoma with distant metastasis. *Pathol Oncol Res* **15**: 167–172.
10. Perner, S, Hofer, MD, Kim, R, Shah, RB, Li, H, Möller, P *et al.* (2007). Prostate-specific membrane antigen expression as a predictor of prostate cancer progression. *Hum Pathol* **38**: 696–701.
11. Liu, H, Moy, P, Kim, S, Xia, Y, Rajasekaran, A, Navarro, V *et al.* (1997). Monoclonal antibodies to the extracellular domain of prostate-specific membrane antigen also react with tumor vascular endothelium. *Cancer Res* **57**: 3629–3634.
12. Samplaski, MK, Heston, W, Elson, P, Magi-Galluzzi, C and Hansel, DE (2011). Folate hydrolase (prostate-specific membrane [corrected] antigen) 1 expression in bladder cancer subtypes and associated tumor neovasculature. *Mod Pathol* **24**: 1521–1529.
13. Haffner, MC, Kronberger, IE, Ross, JS, Sheehan, CE, Zitt, M, Mühlmann, G *et al.* (2009). Prostate-specific membrane antigen expression in the neovasculature of gastric and colorectal cancers. *Hum Pathol* **40**: 1754–1761.
14. Schülke, N, Varlamova, OA, Donovan, GP, Ma, D, Gardner, JP, Morrissey, DM *et al.* (2003). The homodimer of prostate-specific membrane antigen is a functional target for cancer therapy. *Proc Natl Acad Sci USA* **100**: 12590–12595.
15. Aggarwal, S, Singh, P, Topaloglu, O, Isaacs, JT and Denmeade, SR (2006). A dimeric peptide that binds selectively to prostate-specific membrane antigen and inhibits its enzymatic activity. *Cancer Res* **66**: 9171–9177.
16. Tagawa, ST, Beltran, H, Vallabhajosula, S, Goldsmith, SJ, Osborne, J, Matulich, D *et al.* (2010). Anti-prostate-specific membrane antigen-based radioimmunotherapy for prostate cancer. *Cancer* **116** (suppl. 4): 1075–1083.
17. Chen, Z, Penet, MF, Nimmagadda, S, Li, C, Banerjee, SR, Winnard, PT Jr *et al.* (2012). PSMA-targeted theranostic nanoplex for prostate cancer therapy. *ACS Nano* **6**: 7752–7762.
18. Dhar, S, Gu, FX, Langer, R, Farokhzad, OC and Lippard, SJ (2008). Targeted delivery of cisplatin to prostate cancer cells by aptamer functionalized Pt(IV) prodrug-PLGA-PEG nanoparticles. *Proc Natl Acad Sci USA* **105**: 17356–17361.
19. Dhar, S, Kolishetti, N, Lippard, SJ and Farokhzad, OC (2011). Targeted delivery of a cisplatin prodrug for safer and more effective prostate cancer therapy *in vivo*. *Proc Natl Acad Sci USA* **108**: 1850–1855.
20. Gu, F, Langer, R and Farokhzad, OC (2009). Formulation/preparation of functionalized nanoparticles for *in vivo* targeted drug delivery. *Methods Mol Biol* **544**: 589–598.
21. Zhao, Y, Duan, S, Zeng, X, Liu, C, Davies, NM, Li, B *et al.* (2012). Prodrug strategy for PSMA-targeted delivery of TGX-221 to prostate cancer cells. *Mol Pharm* **9**: 1705–1716.
22. Chu, TC, Marks, JW 3rd, Lavery, LA, Faulkner, S, Rosenblum, MG, Ellington, AD *et al.* (2006). Aptamer:toxin conjugates that specifically target prostate tumor cells. *Cancer Res* **66**: 5989–5992.
23. Ni, X, Zhang, Y, Ribas, J, Chowdhury, WH, Castanares, M, Zhang, Z *et al.* (2011). Prostate-targeted radiosensitization via aptamer-shRNA chimeras in human tumor xenografts. *J Clin Invest* **121**: 2383–2390.
24. Dassie, JP, Liu, XY, Thomas, GS, Whitaker, RM, Thiel, KW, Stockdale, KR *et al.* (2009). Systemic administration of optimized aptamer-siRNA chimeras promotes regression of PSMA-expressing tumors. *Nat Biotechnol* **27**: 839–849.
25. Trouet, A and Jollès, G (1984). Targeting of daunorubicin by association with DNA or proteins: a review. *Semin Oncol* **11** (4 suppl. 3): 64–72.
26. Zeman, SM, Phillips, DR and Crothers, DM (1998). Characterization of covalent adriamycin-DNA adducts. *Proc Natl Acad Sci USA* **95**: 11561–11565.
27. Swift, LP, Cutts, SM, Rephaeli, A, Nudelman, A and Phillips, DR (2003). Activation of adriamycin by the pH-dependent formaldehyde-releasing prodrug hexamethylenetetramine. *Mol Cancer Ther* **2**: 189–198.
28. Wang, AH, Gao, YG, Liaw, YC and Li, YK (1991). Formaldehyde cross-links daunorubicin and DNA efficiently: HPLC and X-ray diffraction studies. *Biochemistry* **30**: 3812–3815.

Supplementary Information accompanies this paper on the Molecular Therapy–Nucleic Acids website (http://www.nature.com/mtna)